

Enhanced electroluminescent cooling in GaN-based light-emitting diodes

(invited talk)

Joachim Piprek*

NUSOD Institute LLC, Newark, DE 19714-7204, United States

Zhan-Ming (Simon) Li

Crosslight Software Inc., 230-3410 Loughheed Hwy, Vancouver, BC, V5M 2A4, Canada

Optimized GaN-based light-emitting diodes (LEDs) were recently demonstrated to emit photons of higher energy than provided by the injected electrons up to elevated currents beyond the peak of the power conversion efficiency. Correspondingly, the electrical efficiency is above unity, which is attributed to heat extraction from the crystal lattice. In good agreement with measurements, we investigate the origin of such electroluminescent cooling by advanced numerical simulation including all relevant heat transfer mechanisms. For the first time, our simulations reveal the magnitude and the local profile of the heat extraction from the lattice. The built-in nitride polarization field is found to enhance the cooling effect significantly.

Keywords: light-emitting diode, InGaN/GaN LED, electroluminescent cooling, electroluminescent refrigeration, Peltier cooling

1. INTRODUCTION

For more than a decade, intense research and development efforts have been directed towards improving the electrical-to-optical power conversion efficiency PCE of GaN-based light-emitting diodes (GaN-LEDs), especially for applications in solid state lighting.¹ However, while much attention is devoted to the GaN-LED efficiency droop with higher current,² another phenomenon is hardly discussed in the literature: the surprisingly low turn-on bias of industry-grade devices. A recent paper reports that the photon energy measured at $T = 358\text{K}$ stage temperature is higher than the electron injection energy up to $j = 75\text{ A/cm}^2$ current density and well beyond the peak PCE measured at $j = 3\text{ A/cm}^2$.³ PCE gives the ratio of light output power to electrical input power and it is also called wall-plug efficiency. The high photon energy is attributed to the absorption of thermal power by injected electron-hole pairs before they recombine radiatively.

This electroluminescent cooling phenomenon was first observed in 1953 on SiC diodes and connected to the Peltier effect.⁴ Various investigations followed, some of which theoretically predict the possibility of net LED cooling with $\text{PCE} > 1$ (electroluminescent refrigeration).^{5,6,7} But these models extract the cooling power indirectly from the difference of electrical input power and optical output power so that the Peltier cooling contribution is not identified unambiguously. Only recently, $\text{PCE} > 1$ was demonstrated experimentally for the first time by operating a GaSb-based LEDs with $\lambda = 2150\text{ nm}$ emission wavelength at extremely low bias ($V=70\mu\text{V}$) and elevated temperature ($T=408\text{K}$).⁸ In this low-bias regime, the electrical efficiency $\text{ELE} = E_{\text{ph}}/qV$ can be raised to very high numbers when the bias V approaches zero (E_{ph} – photon energy, q – electron charge). Because all recombination processes respond linearly in this case, the external quantum efficiency EQE remains constant and $\text{PCE} = \text{ELE} \times \text{EQE}$ exceeds unity when the bias is small enough. EQE is the ratio of emitted photon number to injected number of electron-hole pairs and it gives the probability of photon emission. The same group later demonstrated $\text{PCE} > 1$ at room temperature for LEDs with lower bandgap at even smaller bias.⁹

* piprek@nusod.org; phone 1-302-565-4945; www.nusod.org

Large-bandgap GaN-LEDs exhibit a much smaller intrinsic carrier density in the light-emitting active layer and are not expected to achieve $PCE > 1$ in the low-bias regime.⁸ However, a recent publication indicates that electroluminescent cooling of blue GaN-LEDs may lead to performance enhancements at higher stage temperatures.¹⁰ But these results seem to be dominated by a large and temperature-dependent contact resistance, as the measured bias is much higher than in earlier reports on the same device structure.¹¹ Other authors predict $PCE > 1$ for a loss-less GaN-LED up to high current densities; however, their simple model incorrectly assumes that the average photon energy is always several kT higher than the QW transition energy.¹²

2. NUMERICAL MODEL

Utilizing advanced numerical simulation, we here analyze the electroluminescent cooling mechanism in a realistic GaN-LED and directly identify the local distribution and the magnitude of the Peltier cooling power. We employ the advanced LED device simulation software APSYS¹³ which self-consistently computes carrier transport, the wurtzite electron band structure of strained quantum wells (QWs), the photon emission spectrum, as well as heat generation and dissipation. Schrödinger and Poisson equations are solved iteratively in order to account for the quantum well deformation with changing device bias (quantum-confined Stark effect). The carrier transport model includes drift and diffusion of electrons and holes, Fermi statistics, built-in polarization and thermionic emission at hetero-interfaces, as well as Shockley-Read-Hall (SRH) recombination and Auger recombination of carriers.

All relevant heat generation mechanisms are considered self-consistently,¹⁴ i.e., calculated from the local carrier densities and current densities, including Joule heat, heat from non-radiative recombination, as well as the following expression for the Peltier-Thomson heat power¹⁵

$$H_{PT} = -T(\vec{j}_n \nabla P_n + \vec{j}_p \nabla P_p)$$

with the vectors of the current densities \vec{j} and the gradients of the thermopower P for electrons and holes, respectively. The thermopower (Seebeck coefficient) accounts for the excess energy of carriers (in V/K) and it rises with lower carrier density and with higher temperature.¹⁶ Thomson heat is generated when the change in thermopower is caused by a gradient of the internal temperature. Since the net internal heating remains very small in our example below, such Thomson heat is negligible and we here use the term Peltier heat. The thermopower increases when carriers move up a potential barrier, leading to negative Peltier heat (cooling). Positive Peltier heat is generated when carriers drop into a quantum well. More details on our models can be found elsewhere.¹⁷

3. RESULTS AND DISCUSSION

As practical example, our study employs a single-QW blue LED.^{18,19} Since heat removal is expected to be most effective at elevated temperatures, we here refer to the reported case of $T = 400K$ stage temperature.¹⁹ Crucial material parameters are extracted by simultaneously fitting measurements of quantum efficiency, bias, and photon energy vs. current (Fig. 1). The QW interface polarization charge density of $1.3 \times 10^{13} \text{ cm}^{-2}$ is obtained by reproducing the blue-shift of the emission wavelength with rising current which is caused by partial screening of the QW polarization field. Accurate calculation of this polarization field is essential for the extraction of the Peltier cooling power.

The simulated carrier leakage from the QW is negligible in this case and the LED efficiency droop at higher current is solely caused by QW Auger recombination. The low-current efficiency is controlled by defect-related SRH recombination. Our EQE fit in Fig. 1 provides the SRH recombination lifetime of 18ns and the Auger recombination coefficient of $C = 10^{-30} \text{ cm}^6/\text{s}$ which are both close to literature data. The photon generation rate is calculated self-consistently without using the common fit parameter B . The reported photon extraction efficiency is $EXE = 0.465$ and considered constant in our simulation ($EQE = EXE \times IQE$, IQE – internal quantum efficiency).

The fit of the bias-current characteristic in Fig. 1 reveals a contact resistivity of $3 \times 10^{-3} \Omega \text{cm}^2$ for this device which has a negligible influence on our analysis due to the relatively low current density. The simulated bias at low current is slightly higher than measured, possibly due to defect-related tunneling effects²⁰ which are not considered in our model and which may also lead to the slight overestimation of EQE at low current in Fig. 1. However, in good agreement with the measurement, the simulation results in $\text{ELE} > 1$ up to $j = 10 \text{ A/cm}^2$ current density ($I=4\text{mA}$). Since ELE is near unity, the PCE characteristic is almost identical to the EQE curve in Fig. 1. The PCE peak of 0.27 occurs at $\text{ELE} = 1.02$.

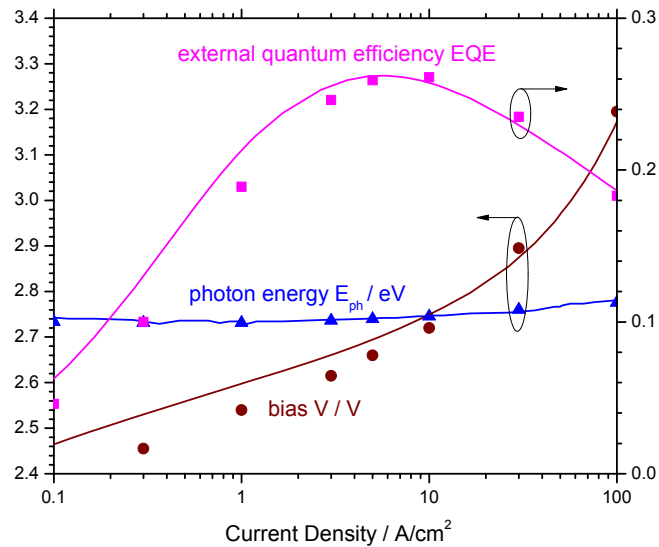


Fig. 1: Comparison between LED measurements (symbols) and simulations (lines) at 400K stage temperature. The LED chip size is $200\mu\text{m} \times 200\mu\text{m}$ and the maximum current is 40mA.

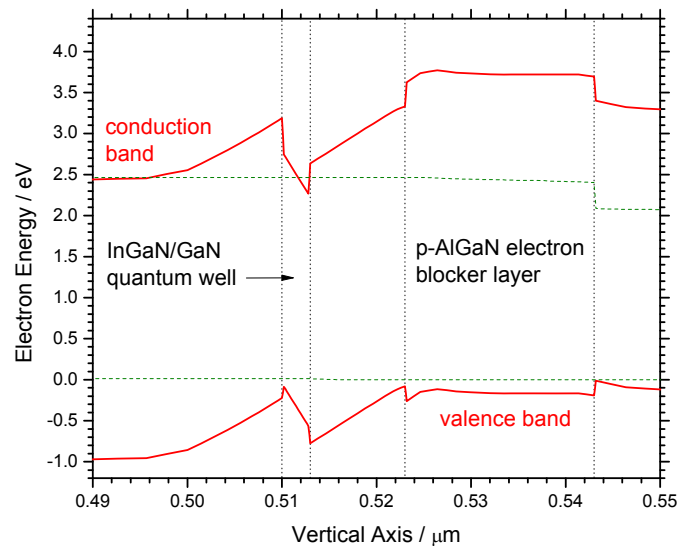


Fig. 2: Energy band diagram near the quantum well (solid: band edges, dashed: quasi Fermi levels).

Figure 2 shows the energy band diagram of the single-quantum-well structure at low current. Built-in polarization causes a strong deformation of the QW and contributes to the triangular potential barrier which electrons and holes need to climb up before entering the QW. The carriers captured in the lowest QW level have a higher energy difference (2.745eV) than the quasi-Fermi levels (2.452eV). This results in the emission of blue photons while the applied bias is still lower than E_{ph}/q , as shown in Fig. 1.

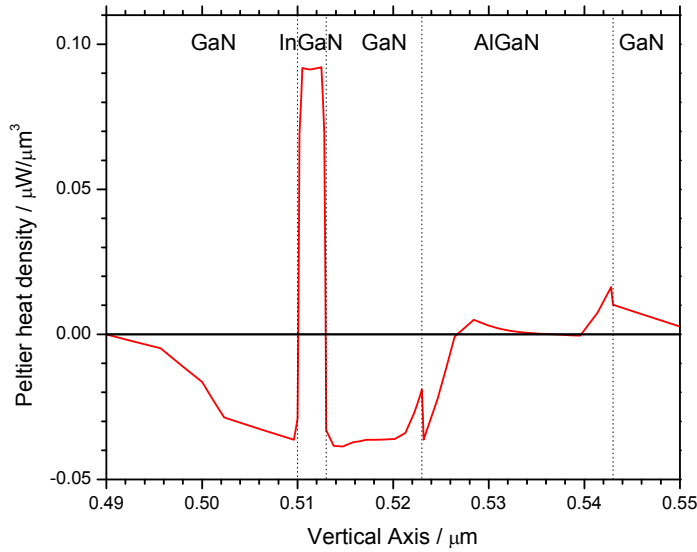


Fig. 3: Vertical Peltier heat profile near the InGaN/GaN quantum well.

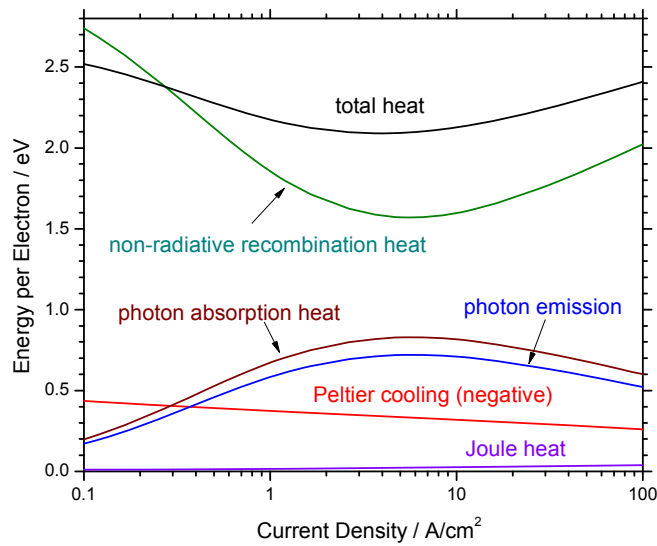


Fig. 4: Energy distribution per injected electron vs. current density.

Carriers climbing up the energy hill towards the QW do so by acquiring thermal energy from the crystal lattice (Peltier cooling). Subsequently, Peltier heating happens when carriers fall into the QW and transfer part of the thermal energy back to the lattice. Figure 3 shows the simulated Peltier heat profile near the QW. Most of the heat extraction occurs in the QW barriers but some also in the AlGaN electron blocking layer (EBL). The net Peltier heat remains negative at all currents. Figure 4 plots the net Peltier cooling energy per injected electron in comparison to other heat

sources. The cooling per carrier slightly declines with higher current since the QW potential barrier is reduced with higher bias. However, the Peltier cooling is substantially smaller than the heating by other mechanism. The strongest heat source is the non-radiative recombination inside the QW, which is dominated by SRH recombination at low currents and by Auger recombination at high currents (for simplicity, we here assume that hot Auger carriers transfer their energy to the lattice within the QW). For intermediate currents, photon generation exhibits the highest probability IQE and the emitted photon energy per injected electron peaks. However, according to the reported light extraction efficiency $EXE = 0.465$, 19 more photons get absorbed internally than emitted from this LED, so that the absorbed energy is larger than the emitted one in Fig. 4. Photon recycling is not considered here.⁷ Joule heat is mainly controlled by the free hole density (10^{18} cm^{-3}) and the hole mobility ($10 \text{ cm}^2/\text{Vs}$) and it remains negligible at our low current density. At the EQE peak of 0.26, the Peltier cooling reduces the total heat power by about 13%. Electroluminescent refrigeration ($PCE > 1$) would require a peak $EQE > ELE^{-1} = 0.98$ in this case.

The internal temperature rise depends on the total thermal resistance R_{th} of the packaged LED. Industry-grade packaging achieves thermal resistances below 10 K/W . We here assume a conservative value of $R_{th} = 60 \text{ K/W}$ and calculate the QW temperature rise with and without Peltier effect (Fig. 5). For this comparison, we remove the Peltier heat (1) from the heat flux equation, but the carriers still gain the same excess energy before dropping into the QW. The maximum self-heating is only 5.8 K and it would rise to 6.7 K without Peltier cooling. For such low temperature rise, the cooling effect on other LED performance parameters is negligible. The EQE characteristics are identical in both cases (see inset of Fig. 5). However, our reference LED is relatively small ($0.2 \text{ mm} \times 0.2 \text{ mm}$). Commercial LEDs are larger and produce more heat so that Peltier cooling is more relevant. Even with a thermal resistance as low as 1 K/W ,²¹ the temperature of a $5 \text{ mm} \times 5 \text{ mm}$ large LED chip would still rise by 60 K at 100 A/cm^2 current density. Furthermore, commercial photon extraction efficiencies are substantially larger than our $EXE = 0.465$ and increase the cooling effect from our 13% to about 20%.²²

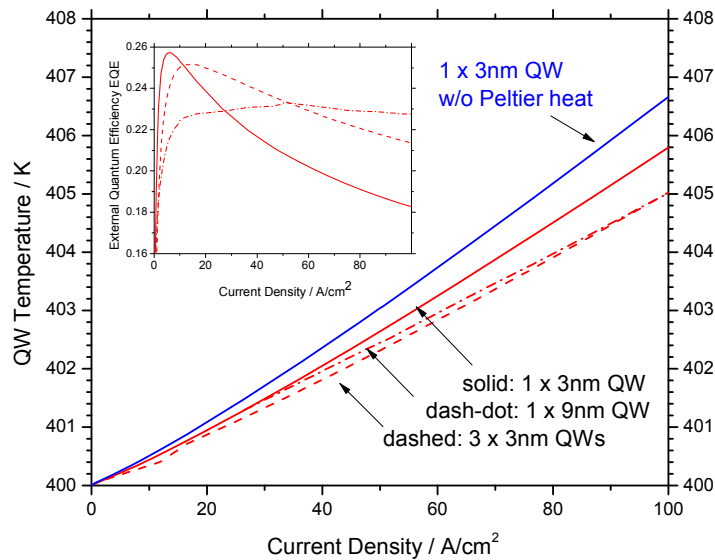


Fig. 5: Quantum well temperature vs. current density as calculated without (solid blue) and with Peltier cooling effect (solid red, dashed: 3 QWs, dash-dot: 9nm thick QW, inset: corresponding external quantum efficiency).

After turning off the built-in polarization in our simulation, the net Peltier cooling power is reduced by about 30% as the missing polarization charges reduce the potential barrier for carriers. In other words, the 13% cooling effect shown in Fig. 5 would be reduced to 9% without polarization. Thus, non-polar or semi-polar nitride LEDs are expected to exhibit less Peltier cooling.

The cooling effect should be higher within LEDs employing multiple QWs since carriers climb up the energy hill towards the QW multiple times. We here add two more QWs to our reference device and show the results in Fig. 6 (dashed lines). The Peltier cooling power clearly rises. However, while most carriers accumulate in the p-side QW, the carrier density in each QW is smaller than in the original LED at any given current, the overall Auger recombination is reduced, the efficiency at higher current is improved (see inset of Fig. 5), and the output power rises. Thus, the reduction in total self-heating (dash-dot line in Fig. 5) is caused both by the increased Peltier cooling and by the reduced Auger recombination.

In comparison, a single 9 nm thick QW produces a slightly reduced Peltier cooling power (dash-dot line in Fig. 6) but the QW carrier density is about three times lower than in the reference LED so that the influence of Auger recombination declines even further. The heat power reduction is almost the same as with 3 QWs but it is now caused by the reduced Auger recombination and not by enhanced Peltier cooling. The EQE droop is almost eliminated (see dash-dot line in inset of Fig. 5). Thus, a promising strategy for reduced heat production at high current is the same as for efficiency droop suppression, namely the reduction of the QW carrier density, which reduces carrier losses.

As figure of merit (FOM) for the Peltier cooling effect, we propose multiplying the absolute cooling power by the probability EQE of photon emission. This FOM gives the cooling power actually extracted from the device independent from other heat sources. The inset of Fig. 6 shows the FOM for all three cases. The multi-QW design clearly wins as it provides the highest cooling power. Making the QW thicker gives a comparable reduction of total heat power, but based on reduced Auger recombination and not caused by larger Peltier cooling.

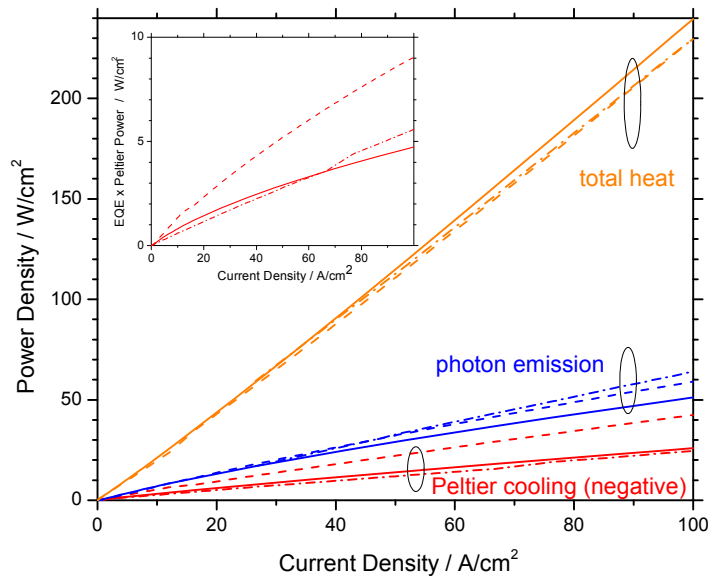


Fig. 6: Peltier cooling power, total heat power, and light output power vs. current density for different active regions (solid: original 3nm QW, dash-dot: 9nm QW, dashed: 3 x 3nm QWs, inset: EQE x Peltier power for all 3 cases).

4. SUMMARY

In conclusion, we have identified the mechanism and the magnitude of electroluminescent cooling in a realistic single-quantum well InGaN/GaN blue LED using advanced device simulation. The built-in polarization field enhances the Peltier cooling from 9% to 13% reduction of the internal temperature rise.

REFERENCES

-
- ¹ Weisbuch, C., et al., *phys. stat. sol. A* 212, 899 (2015)
 - ² Piprek, J., *Appl. Phys. Lett.* 107, 031101 (2015)
 - ³ Hurni, C. A., et al., *Appl. Phys. Lett.* 106, 031101 (2015)
 - ⁴ Lehovec, K., et al., *Phys. Rev.* 89, 20 (1953)
 - ⁵ Han, P., et al., *J. Appl. Phys.* 101, 014506 (2007)
 - ⁶ Heikkilä, O., et al., *J. Appl. Phys.* 107, 033105 (2010)
 - ⁷ Lee, K.C., et al., *J. Appl. Phys.* 111, 014511 (2012)
 - ⁸ Santhanam, P., et al., *Phys. Rev. Lett.* 108, 097403 (2012)
 - ⁹ Santhanam, P., et al., *Appl. Phys. Lett.* 103, 183513 (2013)
 - ¹⁰ Xue, J., et al., *Appl. Phys. Lett.* 107, 121109 (2015)
 - ¹¹ Pan, C. C., et al., *Appl. Phys. Express* 5, 062103 (2012)
 - ¹² David, A., et al., *Appl. Phys. Lett.* 109, 083501 (2016)
 - ¹³ Crosslight Software Inc., Canada (<http://www.crosslight.com>)
 - ¹⁴ Bandelow, U., et al., Ch. 3 in *Optoelectronics Devices – Advanced Simulation and Analysis*, ed. J. Piprek, Springer, New York (2005)
 - ¹⁵ Wolbert, P. B. M., et al., *IEEE Trans. Comput. Aid. Desing* 13, 293 (1994)
 - ¹⁶ Sztejn, A., et al., *J. Appl. Phys.* 113, 183707 (2013)
 - ¹⁷ Piprek, J., *Semiconductor Optoelectronic Devices – Introduction to Physics and Simulation*, Academic Press, San Diego (2003)
 - ¹⁸ Galler, B., et al., *Appl. Phys. Lett.* 101, 131111 (2012)
 - ¹⁹ Galler, B., Ph.D. Thesis, Albert Ludwigs University, Freiburg, Germany (2014)
 - ²⁰ Auf der Maur, M., et al., *Appl. Phys. Lett.* 105, 133504 (2015)
 - ²¹ Humpston, G., *LEDs Magazine* 92, 55-59 (2016)
 - ²² Piprek, J., et al., *Opt. Quant. Electron.* 48, 472 (2016)